IEEE Access
Multidisciplinary | Rapid Review | Open Access Journal

Received 10 June 2023, accepted 27 June 2023, date of publication 30 June 2023, date of current version 7 July 2023.

Digital Object Identifier 10.1109/ACCESS.2023.3291209

RESEARCH ARTICLE

Adaptive Fuzzy Output Feedback Control Design for Pneumatic Active Suspension With Unknown Dead Zone

CONG MINH HO[1] AND KYOUNG KWAN AHN[2], (Senior Member, IEEE)
[1]Faculty of Mechanical Engineering, Ho Chi Minh City University of Technology and Education, Ho Chi Minh City 70000, Vietnam
[2]School of Mechanical and Automotive Engineering, University of Ulsan, Ulsan 44610, South Korea

Corresponding author: Kyoung Kwan Ahn (kkahn@ulsan.ac.kr)

This work was supported in part by the Basic Science Program through the National Research Foundation of Korea (NRF) funded by the Ministry of Science and ICT, South Korea, under Grant NRF 2020R1A2B5B03001480; and in part by the Regional Innovation Strategy (RIS) through NRF funded by the Ministry of Education (MOE) under Grant 2021RIS-003.

ABSTRACT This study proposes an adaptive fuzzy state observer-based command filtering technique for a pneumatic active suspension considering the effects of uncertain parameters, unmeasured states, and non-ideal characteristics of the air spring actuator. Firstly, a mathematical model is constructed to investigate the dynamic behavior and examine external disturbances and system errors. The problems of input saturation and unknown dead zone are also considered in this work. By using fuzzy logic systems, unknown nonlinear functions of parametric uncertainties and various passenger masses are approximated. Then, a serial-parallel state observer is designed not only to estimate unmeasured state variables of the suspension system but also to eliminate the prediction errors of observer estimation. To enhance the suspension performance, a prescribed performance function (PPF) is applied to ensure the convergence rate of vertical displacement within specified boundaries. Besides, the "explosion of complexity" issue is eliminated by employing the command filtering technique. An adaptive fuzzy output feedback controller is then developed to reduce the tracking error of sprung mass displacement under the effect of unknown parameters, unmeasured states, and a non-ideal actuator. Moreover, the Lyapunov theorem is applied to prove the stability of the designed controller. Finally, comparative simulation examples will help verify the effectiveness and reliability of the developed approach.

INDEX TERMS Active suspension systems (ASSs), fuzzy logic systems (FLSs), serial-parallel observer, prescribed performance control (PPC), command filtered control (CFC).

I. INTRODUCTION

Pneumatic active suspension systems have been widely used in modern automobile technology as they can provide variable stiffness coefficients and flexible active force to dissipate the external excitations caused by irregular road profiles [1]. Compared with hydraulic or electromagnetic actuators [2], [3], a pneumatic spring has performed advantages of low cost, cleanliness, and high power-to-weight ratio characteristics [4], [5]. However, nonlinearity is one of the main disadvantages of pneumatic suspension which makes it challenging to establish a precise mathematical model and design a control algorithm. To solve this problem, many advanced controllers have been proposed to increase suspension performance such as adaptive [6], output feedback [7], finite-time [8], and sliding mode control [9]. Vaijayanti et al. [10] designed a nonlinear control to satisfy the suspension objectives of ride comfort and driving safety. To investigate the problem of time delay and output constraint, Li et al. [11] designed a fuzzy output feedback controller for a vehicle suspension system. Rath et al. [12] developed a robust sliding mode controller considering nonlinear parameters to limit the chassis movement of the hydraulic suspension model. However, chattering and

The associate editor coordinating the review of this manuscript and approving it for publication was Yiming Tang.

singularity problems in the control law are potential limitations associated with SMC approaches [13]. To stabilize the sprung mass displacement with the effects of uncertain parameters, the backstepping control is designed for the nonlinear active suspension to get ride comfort [14]. Nonetheless, these control designs assumed that ideal actuators were investigated while actuator dynamics were ignored. Besides, the problems of chassis displacement have not been fully considered under the presence of unknown parameters and unmodeled dynamics of pneumatic suspension.

Although the majority of most previous studies can ensure the asymptotic stability of the suspension system, the convergence rate of tracking error of vertical displacement cannot be seriously considered. Unfortunately, it may lead to handling instability, and driving safety cannot be ensured if this constraint bound is violated. To satisfy the output constraint, a PPF was introduced by Bechlioulis et al. [15], which can converge the tracking error to zero in the steady state and guarantee the maximum overshoot. Huang et al. [16] designed an adaptive control-based PPF to stabilize the vertical displacement and improve passenger comfort. Combining the prescribed performance with an adaptive controller, Liu et al. [17] ensured the chassis displacement and pitch angle of the suspension system with model uncertainty. Nonetheless, these above control schemes have difficulties in handling stability and driving safety [18]. Besides, most above studies are designed based on the conventional backstepping algorithm which cannot solve the explosion of complexity issues caused by repeating derivations of virtual controllers. As an alternative method, a CFC scheme can eliminate this problem by adopting the outputs of command filters to avoid using the differentiation of the intermediate control signal at each step [19], [20]. Besides, CFC can improve control performance by employing an error compensation mechanism to minimize the errors of the command filters [21]. So far, however, a few studies have applied the CFC for the pneumatic suspension considering model uncertainties and unmeasured states [20].

Generally, suspension systems always contain unmodeled dynamics and external disturbances, however, these unknown parameters are assumed to be linear in almost previous research. Thus, the control performance will degrade if these inevitable factors are neglected. Recently, FLSs [22] and neural networks (NNs) have been increasingly employed to model and control uncertain suspension systems [23]. Zhang et al. [24] proposed an adaptive dynamic surface controller in which the unknown functions are addressed by NNs to ensure the vertical constraint of the sprung mass. To approximate the parametric uncertainties of nonlinear suspension, Li et al. [25] designed an adaptive event-triggered fuzzy control that can solve the actuator failure and improve the ride comfort. It should be noted that the mentioned control schemes are all suitable for the ASSs where the system states are completely known, and actuator dynamics are ignored. The results in [26] required that all state variables of the system dynamics be directly measured even though they are usually immeasurable or difficult to define. To design the output feedback control in the case of unmeasured system states, an adaptive state observer based on intelligent techniques was developed in [27], [28], [29]. Pan et al. [7] proposed an output feedback finite-time control to approximate parametric uncertainties and unknown states for active suspension. Nonetheless, the aforementioned studies did not pay attention to improving the approximation performance. Moreover, the problem of the unmodeled dynamic and non-ideal actuator should be carefully investigated to enhance the high accuracy of pneumatic suspension.

In practical applications, hysteresis, backlash, and dead zone are three generally unknown non-smooth characteristics of actuators, which degrade control performance and even cause system instability [30], [31]. Particularly, dead zone nonlinearities always exist in pneumatic suspension systems because of the response characteristic of proportional control valves. Nevertheless, in fact, most suspension controllers are considered ideal actuators for system modeling and ignore these uncertainties. Hua et al. [32] proposed a novel adaptive controller for a half-car active suspension to overcome the adverse effects of the dead-zone problem. To compensate for the effects of dead-zone and hysteresis actuator, Pan et al. [6] designed an adaptive tracking control scheme to improve ride comfort and handling stability. Besides, most previous studies of ASSs ignored the input saturation problem of pneumatic suspension, however, the control performance depends on the limitation of the input control signal. For this purpose, some FLSs or NNs approximation techniques are employed to deal with the effects of dead zone and saturation. Zhang et al. [33] developed a novel fuzzy sliding mode control to guarantee the ride comfort of half-car suspension considering an unknown dead zone and actuator saturation. However, none of the results of studies considered the dead-zone actuator of pneumatic active suspension under the presence of unmeasurable states, which are considered in this study.

Based on the above summary, we propose an adaptive fuzzy observer output feedback control to improve the control performance of the pneumatic suspension with unknown parameters, input saturation, and dead zone characteristics. Firstly, a mathematical model of the air spring actuator is contributed based on thermodynamic theory to investigate the suspension behavior. To mitigate the effect of the actuator nonlinearities, the inverse dynamic functions are employed for the dead zone and input saturation problems. However, it is difficult to design the ideal controller to stabilize the sprung mass under the effects of unmodeled dynamics, external disturbances, and different masses of passengers. Besides, due to unmeasurable variables of chassis velocity and internal pressure of air spring, all system states become unavailable for controller design. Therefore, FLSs are applied to approximate unknown continuous functions caused by parametric uncertainties while a fuzzy state observer is then proposed to approximate unmeasured variables. Compared with a general observer, a serial-parallel approximation technique was constructed while the prediction errors of the state observation model are considered in this design. Thus, the control algorithm is designed with a smoother parameter adaptation which can improve the faster state tracking and better parameter convergence. Besides, by constructing a PPF constraint, the proposed scheme can enhance the convergence rate and guarantee the maximum overshoot of tracking error to stabilize the chassis displacement. Finally, with the help of the CFC technique, the issue of the explosion complexity of traditional backstepping is eliminated. The main contributions of this research are described as follows.

1. An adaptive output feedback control is proposed for the pneumatic suspension to guarantee the chassis stability under the presence of uncertain parameters, unmeasurable states, input saturation, and dead zone actuator.
2. The serial-parallel approximation model based on the fuzzy observer technique is designed to approximate unmeasured variables while the prediction errors are incorporated with the developed scheme to enhance better control performance.
3. PPF and CFC techniques not only ensure the tracking error of chassis displacement but also eliminate the explosion of complexity issue of conventional backstepping.

The remainder of the manuscript is arranged as follows. The pneumatic suspension descriptions and actuator characteristics of the quarter vehicle are described in Section II. An adaptive output feedback CFC scheme with PPF based on a serial-parallel observer will be proposed in Section III. Then, the stability of the closed-loop system is proved. Moreover, the comparative simulations are performed in section IV to verify the efficiency of the designed method. Finally, some conclusions about pneumatic suspension are given in Section V.

II. PNEUMATIC SUSPENSION DESCRIPTION AND PRELIMINARIES

The quarter model of pneumatic active suspension with air bellow is described in Fig. 1. In this design, the sprung mass m_s denotes the weight of the chassis and the total mass of the passengers. The mechanical assembly of the suspension structure is expressed by the unsprung mass m_u. To define the sprung mass and unsprung mass positions, symbols z_s and z_u are used while the disturbance of road profile is denoted by z_r. The stiffness and damping coefficients of spring and damper are described by k_s and c_a, respectively. Besides, k_{st}, c_{at} are stiffness coefficient and damper values of the tire. To provide an active force to dissipate external excitation, a pneumatic spring with the stiffness coefficient k_p is placed between the sprung mass and unsprung mass.

Besides, the nonlinearity model of pneumatic spring contains parametric uncertainties caused by the twisted-wire rubber material under the effect of external forces. Thus, the dynamic model of the pneumatic spring must consider these parametric deviations, which will be detailed in this study. The dynamic equations of the quarter ASSs are described based on [22].

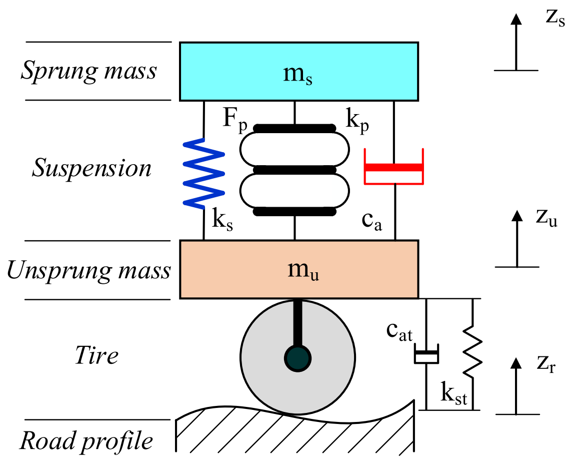

FIGURE 1. Pneumatic active suspension model.

As we know the air spring can provide a flexible force for regulating the sprung mass to get passenger comfort. However, the dissipation of vibration capacity should be carefully considered due to the limitation of the pneumatic system. Hence, the characteristic of input saturation is examined in this study. The definition of actuator saturation can be expressed by

$$u^s = sat(u) = \begin{cases} u, & |u| < u_L \\ u_L sign(u), & |u| \geq u_L \end{cases} \tag{1}$$

where u^s is the saturation signal and u_L is the known boundary.

Generally, the saturation nonlinearity (1) cannot be directly used in the controller design because of the sharp corners $u = u_L$. To solve this drawback, a Gaussian error function is applied to indicate the input saturation signal as follows

$$u^s = sat(u) = u^E \times erf\left(\frac{\sqrt{\pi}}{2u^E}u\right) \tag{2}$$

where $u^E = u_L sign(u)$ and $erf(x)$ is the Gauss error function.

Definition 1 [34]: Gauss error function is a continuously differentiable function, which is used to express a nonelementary function of sigmoid shape

$$erf(x) = \frac{2}{\sqrt{\pi}} \int_0^x e^{-t^2} dt \tag{3}$$

To apply the input saturation for the control design, we obtain the output signal u^s as [35]

$$u^s = h_u u + d(u) \tag{4}$$

where h_u is the smooth function and $d(u)$ is bounded by $|d(u)| \leq \Delta$.

On the other hand, the dead zone phenomenon often occurs in the pneumatic system because most proportional valves are commonly designed to clog the orifice. Hence, there is an overlapping phenomenon of the valve spool at the null condition. This will keep the output constant until the control signal magnitude is over a threshold value. Then, the actual opening of the orifice area can be considered as dead-zone nonlinearity, which is expressed by

$$u = DZ(u_d^s(t)) \tag{5}$$

where DZ denotes the dead zone operator and $u_d^s(t)$ is the input nonlinearity. Based on [36], we can write

$$DZ\left(u_d^s(t)\right) = \begin{cases} k_a\left(u_d^s(t) - q_a\right), & \text{for } u_d^s(t) \geq q_a \\ 0, & \text{for } -q_b < u_d^s(t) < q_a \\ k_b\left(u_d^s(t) + q_b\right), & \text{for } u_d^s(t) \leq -q_b \end{cases} \tag{6}$$

where $k_b > 0$ and $k_a > 0$ are the left and right slope of the dead zone while $q_b > 0$ and $q_a > 0$ are the dead zone parameters, respectively. To simplify the control design, the dead zone can be transferred by

$$u = k(t)u_d^s(t) + q(t) \tag{7}$$

$$k(t) = \begin{cases} k_a, & \text{if } u_d^s(t) > 0 \\ k_b, & \text{if } u_d^s(t) \leq 0 \end{cases} \tag{8}$$

$$q(t) = \begin{cases} -k_a q_a, & \text{for } u_d^s(t) \geq q_a \\ -k(t)u_d(t), & \text{for } -q_b < u_d^s(t) < q_a \\ k_b q_b, & \text{for } u_d^s(t) \leq -q_b \end{cases} \tag{9}$$

For a practical system, the dead zone parameters k_b, k_a, and $q\,(t)$ are bounded. Hence, we can obtain

$$\begin{cases} \min\,(k_a, k_b) \leq |k\,(t)| \leq \max\,(k_a, k_b) \\ \min\,(k_a q_a, k_b q_b) \leq |q\,(t)| \leq \max\,(k_a q_a, k_b q_b) \end{cases} \tag{10}$$

Finally, considering the actuator characteristics (4), (7), and unmodeled parameters of air bellow, we establish the full dynamic equations for the quarter pneumatic suspension as

$$\begin{aligned} \dot{x}_1 &= x_2 + d_1\,(t) \\ \dot{x}_2 &= x_5 + \frac{1}{m_s}\left[-k_s(x_1 - x_3) - c_a(x_2 - x_4)\right] + d_2\,(t) \\ \dot{x}_3 &= x_4 \\ \dot{x}_4 &= \frac{1}{m_u}\begin{bmatrix} -k_{st}(x_3 - z_r) - c_{at}(x_4 - \dot{z}_r) + k_s(x_1 - x_3) \\ +c_a(x_2 - x_4) - m_s x_5 - m_s d_2 \end{bmatrix} \\ \dot{x}_5 &= \frac{\kappa RT}{m_s\,(z_{as0} + x_1 - x_3)}\sigma_{sv} q_{as}\left(h_u\left(k u_d^s + q\right) + d\right) \\ &\quad - \frac{\gamma}{(z_{as0} + x_1 - x_3)}\,(x_2 - x_4)\,x_5 + p\,(t) \end{aligned} \tag{11}$$

where $d_1\,(t)$ is the position error of chassis displacement and $p\,(t)$ is the time-varying modeling error of pneumatic spring which contains unmodeled dynamics and unknown parameters.

Besides, the nonlinearity model of pneumatic spring contains parametric uncertainties caused by the twisted-wire rubber material under the effect of external forces. Thus, the dynamic model of the pneumatic spring must consider these parametric deviations, which will be detailed in the next section.

To guarantee passenger comfort, the active suspension must dissipate the external vibrations that cause excitation to the sprung mass. Then, the controller design will concentrate on the mechanical equations of the chassis by

$$\begin{aligned} \dot{x}_1 &= f_1 + g_1 x_2 + d_1\,(t) \\ \dot{x}_2 &= f_2 + g_2 x_5 + d_2\,(t) \\ \dot{x}_5 &= f_3 + g_3 u_d^s + d_3\,(t) \end{aligned} \tag{12}$$

where $f_1 = 0$ $f_2 = 1/m_s[-k_s(x_1 - x_3) - c_a(x_2 - x_4)]$, $f_3 = [-\kappa/(z_{as0} + x_1 - x_3)](x_2 - x_4)x_5$, $g_1 = 1$, $g_2 = 1$, $g_3 = \{\kappa RT/[m_s(z_{as0} + x_1 - x_3)]\}\sigma_{sv} q_{as} h_u k(t)$, $d_3(t) = p(t) + g_3 q(t)/k(t) + g_3 d(u)/\,(h_u k(t))$.

Obviously, it can be concluded from the general dynamic model (12) that f_2 and f_3 are unknown nonlinear functions since state variables x_3 and x_4 are disregarded in the control algorithm. Therefore, the suspension control performance will be degraded if these unknown parameters are neglected. To enhance the control objective under the above problems, some following assumptions and lemmas are suggested.

Assumption 1: $d_i\,(t)\,, i = 1, 2, 3$ is the unknown bounded time-varying disturbance and satisfies $|d_i\,(t)| \leq \bar{D}_i$, $i = 1, 2, 3$.

Besides, to estimate unknown nonlinear functions caused by parametric uncertainties, the fuzzy approximation technique is employed. There are four parts of FLSs structure: fuzzifier, fuzzy rule base, fuzzy inference engine, and defuzzifier. The knowledge-based consists of a series of If-Then rules as follows

$$R^l\text{: If} x_1 \text{ is } E_1^l \text{ and } x_2 \text{ is } E_2^l \text{ and} \ldots x_n \text{ is } E_n^l, \quad \text{then } y \text{ is } F^l, l = 1, \ldots, N \tag{13}$$

where $X = [x_1, x_2, l, x_n]^T$ is FLSs input while y represents FLSs output; E_i^l and F^l denote fuzzy sets corresponding with fuzzy membership functions $\mu_{E_i^l}\,(x_i)$ and $\mu_{F^l}\,(y)$; and N denotes for the total of fuzzy rules.

Applying singleton fuzzifier, center average defuzzification, and product inference, FLSs are defined by

$$y\,(X) = \frac{\sum_{l=1}^N \bar{y}_l \prod_{i=1}^n \mu_{E_i^l}\,(X_i)}{\sum_{l=1}^N \left(\prod_{i=1}^n \mu_{E_i^l}\,(X_i)\right)} \tag{14}$$

where $\bar{y}_l = \max\limits_{y \in R}\left\{\mu_{F^l}\,(y)\right\}$.

Thus, we can receive the fuzzy basic function

$$s_l = \frac{\prod_{i=1}^n \mu_{E_i^l}\,(X_i)}{\sum_{l=1}^N \left(\prod_{i=1}^n \mu_{E_i^l}\,(X_i)\right)} \tag{15}$$

From (14), the fuzzy logic approximation is determined by

$$y\,(X) = \theta^T S\,(X) \tag{16}$$

where $S(X) = [s_1(X), s_2(X), \ldots, s_N(X)]^T$ denote the basis function vector and $\theta^T = [\bar{y}_1, \bar{y}_2, \ldots, \bar{y}_N] = [\theta_1, \theta_2, \ldots, \theta_N]$.

Lemma 1 [37]: Determine any continuous vector function $f\,(X)$ on a compact set Ω, there exists a positive constant

$\eta > 0$ satisfying the FLSs estimation

$$\sup_{X\in\Omega}\left|f(X) - \theta^T S(X)\right| \le \eta \tag{17}$$

where θ is the ideal FLSs weight matrix, η is an error value of the fuzzy approximation in comparison with an unknown function, and $S(X)$ is bounded by a positive constant λ, $\|S(X)\| \le \lambda$.

In this study, unknown functions $f(X)$ determined on the compact set $X \in \Omega$ will be approximated by the FLSs technique

$$f_i(X) = \theta_i^T S_i(X_i) + \eta_i \tag{18}$$

Lemma 2 [19]: The command filtered theory is applied to eliminate the explosion of complexity issues caused by the derivative of virtual controllers

$$\begin{aligned}\dot{\xi}_{i1} &= \rho_m \xi_{i2}\\ \dot{\xi}_{i2} &= -2\rho_m o_m \xi_{i2} - \rho_m(\xi_{i1} - \alpha_{i-1})\end{aligned} \tag{19}$$

where $x_i^c = \xi_{i1}$ and $\dot{x}_i^c = \dot{\xi}_{i1}$ are the output of each filter designed to determine tracking error $e_i = x_i - x_i^c$, ρ_m and o_m the control parameters while α_{i-1} denotes the intermediate signal. When the input signal α_{i-1} and their derivatives are bounded by $|\dot{\alpha}_{i-1}| \le \ell_1$ and $|\ddot{\alpha}_{i-1}| \le \ell_2$, there exist $o_m \in (0, 1]$ and $\rho_m > 0$ satisfied the following inequality

$$\left|x_i^c - \alpha_{i-1}\right| \le \ell_3 \tag{20}$$

where $\ell_i > 0, i = 1, 2, 3$ are positive parameters.

Remark 1: The command filter technique (19) can estimate the virtual control signal x_i^c and $\dot{x}_i^c$ without differentiation. Therefore, the issue of "explosion of complexity" in the traditional backstepping control can be dismissed.

Lemma 3 [19]: The errors of the command filtered control $(\theta_{i1} - \alpha_{i-1})$ is removed by the compensation mechanisms μ_i

$$\begin{aligned}\dot{\mu}_1 &= -k_1\mu_1 + g_1\mu_2 + g_1\left(x_2^c - \alpha_1\right)\\ \dot{\mu}_i &= -k_i\mu_i - g_{i-1}\mu_{i-1} + g_i\mu_{i+1} + g_i\left(x_{i+1}^c - \alpha_i\right)\\ \dot{\mu}_n &= -k_n\mu_n - g_{n-1}\mu_{n-1}\end{aligned} \tag{21}$$

where k_i are control parameters and the initial condition is chosen $\mu_i(0) = 0$ for $t \in [0, T_1]$. The compensation mechanisms are bounded by invoking [38]

$$\|\mu_i(t)\| \le \frac{\ell_3 \bar{G}_{31}}{2k_0}\left(1 - e^{-2k_0(t-T_1)}\right) \tag{22}$$

where $k_0 = (1/2)\, min(k_i)$ and $|g_3| \le \bar{G}_{31}$.

Control objectives: The control design is developed to guarantee three objectives of pneumatic suspension

1) *Ride comfort:* The proposed method can stabilize the chassis movement to isolate passengers from continuous excitation of road disturbances.
2) *Handling stability:* This objective limits the suspension deflection to the maximum allowable space of the mechanical structure. It means that the relative suspension deflection (RSD) must be smaller than 1.

$$RSD = \frac{z_s - z_u}{z_M} \tag{23}$$

where z_M is the maximum sprung mass displacement.
3) *Driving safety:* This standard ensures that the tire is in continuous contact with the road surface. For this purpose, the relative tire fore (RTF) is kept at less than 1.

$$RTF = \frac{F_{st} + F_{at}}{[m_s + m_u]\, g} \tag{24}$$

Remark 2: It is challenging to design a novel controller that can satisfy these suspension requirements since improving the passenger comfort will require larger suspension deflection and reduce the road holding objective. This proposed control can ensure three objectives by employing the PPF technique.

III. ADAPTIVE FUZZY OUTPUT FEEDBACK CONTROL WITH PPF AND SERIAL-PARALLEL OBSERVER

A. FUZZY SERIAL-PARALLEL STATE OBSERVER

To overcome this drawback of unmeasured states, a serial-parallel approximation technique was developed in this section. Firstly, a fuzzy state observer is proposed to approximate unmeasurable states. Then, the prediction errors are solved by the serial-parallel estimation model. Hence, the proposed observer can improve the tracking performance for control design as it can estimate unmeasured states and eliminate estimation errors. Now, the system dynamics (12) can be converted into the following general form

$$\begin{aligned}\dot{x} &= Ax + Ky + B_1 f_1(\bar{x}_1) + B_2 f_2(\bar{x}_2) + B_3 f_3(\bar{x}_3)\\ &\quad + B_3 g_3(\bar{x}_1)\, u_d^s\\ y^f &= Cx\end{aligned} \tag{25}$$

where $x = [x_1, x_2, x_5]^T$, $\bar{x}_2 = [x_1, x_2]^T$, $\bar{x}_3 = [x_1, x_2, x_5]^T$

$$A = \begin{bmatrix} -a_1 & 1 & 0\\ -a_2 & 0 & 1\\ -a_3 & 0 & 0\end{bmatrix}; \quad B_1 = [1, 0, 0]^T;\ B_2 = [0, 1, 0]^T;$$
$$B_3 = [0, 0, 1]^T; \quad C = [1, 0, 0];\ K = [a_1, a_2, a_3]^T$$

According to Lemma 1, FLSs are applied to estimate unknown nonlinear functions $f_i(\bar{x}_i)$, $i = 1, 2, 3$ and $g_3(\bar{x}_1)$ via $\hat{f}_i(\bar{x}_i|\theta_i) = \theta_i^T S_i(\bar{x}_i)$, $\hat{g}_3(\bar{x}_1|\theta_G) = \theta_G^T S_G(\bar{x}_1)$ by

$$f_i(\bar{x}_i) = \hat{f}_i\left(\bar{x}_i|\theta_i^*\right) + \varepsilon_i = \theta_i^{*T} S_i(\bar{x}_i) + \varepsilon_i \tag{26}$$

$$g_3(\bar{x}_1) = \hat{g}_3\left(\bar{x}_1|\theta_G^*\right) + \varepsilon_G = \theta_G^{*T} S_G(\bar{x}_1) + \varepsilon_G \tag{27}$$

where θ_i and θ_G are the estimations of the ideal weights θ_i^*, θ_G^*

$$\theta_i^* = \arg\min_{\theta_i\in\Omega_i}\left[\sup_{\bar{x}_i\in U_i}\left|\hat{f}_i\left(\hat{\bar{x}}_i|\theta_i\right) - f_i\left(\hat{\bar{x}}_i\right)\right|\right]$$

$$\theta_G^* = \arg\min_{\theta_G\in\Omega_G}\left[\sup_{\bar{x}_G\in U_G}\left|\hat{g}_3\left(\hat{\bar{x}}_1|\theta_G\right) - g_3\left(\hat{\bar{x}}_1\right)\right|\right]$$

where Ω_i and U_i are the compact regions of θ_i and $\bar{x}_i$.

The minimum fuzzy approximation errors ε_i and ε_G are determined by

$$\begin{aligned}\varepsilon_i &= f_i(\bar{x}_i) - \hat{f}_i(\bar{x}_i|\theta_i^*)\\ \varepsilon_G &= g_3(\bar{x}_1) - \hat{g}_3(\bar{x}_1|\theta_G^*)\end{aligned} \tag{28}$$

Assumption 2: There are positive constants ε_i^* and ε_G^* satisfying $\|\varepsilon_i\| \le \varepsilon_i^*$ and $\|\varepsilon_G\| \le \varepsilon_G^*$.

A normal state observer with the FLSs technique can be proposed to estimate unmeasurable system variables (25)

$$\begin{aligned}\dot{\hat{x}}_1 &= \hat{x}_2 + \hat{f}_1\left(\hat{\bar{x}}_1|\theta_1\right) + a_1(x_1 - \hat{x}_1)\\ \dot{\hat{x}}_2 &= \hat{x}_5 + \hat{f}_2\left(\hat{\bar{x}}_2|\theta_2\right) + a_2(x_1 - \hat{x}_1)\\ \dot{\hat{x}}_5 &= \hat{g}_3\left(\hat{\bar{x}}_1|\theta_G\right)u_d^s + \hat{f}_3\left(\hat{\bar{x}}_3|\theta_3\right) + a_3(x_1 - \hat{x}_1)\end{aligned} \tag{29}$$

The general form of state observer (29) can be written by

$$\begin{aligned}\dot{\hat{x}} = A\hat{x} + Ky + B_1\hat{f}_1(\bar{x}_1|\theta_1) + B_2\hat{f}_2(\bar{x}_2|\theta_2) + B_3\hat{f}_3\left(\hat{\bar{x}}_3|\theta_3\right)\\ + B_3\hat{g}_3\left(\hat{\bar{x}}_1|\theta_G\right)u_d^s\end{aligned} \tag{30}$$

where $\hat{x} = [\hat{x}_1, \hat{x}_2, \hat{x}_5]^T$ is defined to estimate x.

Let $\tilde{x}_i = x_i - \hat{x}_i = [\tilde{x}_1, \ldots, \tilde{x}_i]$ as the observer error. Then, the observer error is defined based on (25) and (30) as follows

$$\begin{aligned}\dot{\tilde{x}} &= A\tilde{x} + B_1\left(f_1(\bar{x}_1) - \hat{f}_1\left(\hat{\bar{x}}_1|\theta_1\right)\right)\\ &\quad + B_2\left(f_2(\bar{x}_2) - \hat{f}_2\left(\hat{\bar{x}}_2|\theta_2\right)\right)\\ &\quad + B_3\left(f_3(\bar{x}_3) - \hat{f}_3\left(\hat{\bar{x}}_3|\theta_3\right)\right)\\ &\quad + B_3\left(g_3(\bar{x}_1) - \hat{g}_3\left(\hat{\bar{x}}_1|\theta_G\right)\right)u_d^s + D\\ &= A\tilde{x} + \sum_{i=1}^{3} B_i\delta_i + B_3\delta_G u_d^s + D\end{aligned} \tag{31}$$

where $D = [d_1(t), d_2(t), d_3(t)]^T$ and δ_i, δ_G denotes fuzzy approximation errors which can be calculated by

$$\begin{aligned}\delta_i &= f_i(\bar{x}_i) - \hat{f}_i\left(\hat{\bar{x}}_i|\theta_i\right)\\ \delta_G &= g_3(\bar{x}_1) - \hat{g}_3\left(\hat{\bar{x}}_1|\theta_G\right)\end{aligned} \tag{32}$$

From (26) and (27), we can write (32) as follows

$$\delta_i = \theta_i^{*T}\left(S_i(\bar{x}_i) - S_i\left(\hat{\bar{x}}_i\right)\right) + \tilde{\theta}_i^T S_i\left(\hat{\bar{x}}_i\right) + \varepsilon_i \tag{33}$$

$$\delta_G = \theta_G^{*T}\left(S_G(\bar{x}_1) - S_G\left(\hat{\bar{x}}_1\right)\right) + \tilde{\theta}_G^T S_G\left(\hat{\bar{x}}_1\right) + \varepsilon_G \tag{34}$$

Assumption 3: Define $\upsilon_i = \varepsilon_i - \delta_i$, $\upsilon_G = \varepsilon_G - \delta_G$. There are positive constants υ_i^* and υ_N^* satisfying $\|\upsilon_i\| \le \upsilon_i^*$ and $\|\upsilon_G\| \le \upsilon_G^*$.

From (31), there are errors between system states and estimation values that cannot be solved by the above estimation technique. Hence, a serial-parallel observer is designed by

$$\begin{aligned}\dot{\hat{\hat{x}}}_1 &= \hat{x}_2 + \hat{f}_1\left(\hat{\bar{x}}_1|\theta_1\right) + \varpi_1\left(\hat{x}_1 - \hat{\hat{x}}_1\right)\\ \dot{\hat{\hat{x}}}_2 &= \hat{x}_5 + \hat{f}_2\left(\hat{\bar{x}}_2|\theta_2\right) + \varpi_2\left(\hat{x}_2 - \hat{\hat{x}}_2\right)\\ \dot{\hat{\hat{x}}}_5 &= \hat{g}_3\left(\hat{\bar{x}}_1|\theta_G\right)u_d^s + \hat{f}_3\left(\hat{\bar{x}}_3|\theta_3\right) + \varpi_3\left(\hat{x}_3 - \hat{\hat{x}}_3\right)\end{aligned} \tag{35}$$

where $\varpi_1, \varpi_2, \varpi_3$ are designed parameters.

Then, the prediction error is defined by

$$\nu_i = \hat{x}_i - \hat{\hat{x}}_i \tag{36}$$

Substituting (29) and (35) into (36), we obtain

$$\dot{\nu}_i = a_i(x - \hat{x}_1) - \varpi_i\left(\hat{x}_i - \hat{\hat{x}}_i\right) \tag{37}$$

B. ADAPTIVE FUZZY OUTPUT FEEDBACK CONTROL WITH PRESCRIBED PERFORMANCE AND SERIAL-PARALLEL OBSERVER

This section presents a novel command filtered control law based on the modified backstepping technique. Besides, the Lyapunov theorem is employed to examine the stability of the developed method and prove the convergence of the observer.

Step 1: In this step, the PPF is employed to guarantee the sprung mass displacement within the boundary constraint. Firstly, the tracking error of x_1 is determined by

$$e_1 = x_1 - x_d \tag{38}$$

where x_d is the desired trajectory.

Definition 2: A PPF is defined by a positive smooth function

$$\lambda(t) = (\lambda_0 - \lambda_\infty)e^{-\gamma t} + \lambda_\infty \tag{39}$$

where $\gamma > 0$ describes the convergence rate, λ_0 is the initial constraint, and λ_∞ denotes the allowable steady-state error, which are selected to satisfy the initial conditions $\lim_{t\to 0}\lambda(t) = \lambda_0 > 0$, $\lim_{t\to\infty}\lambda(t) = \lambda_\infty > 0$, and $\lambda_0 > \lambda_\infty$.

According to (39), the constraint condition is transformed by the following inequality

$$-\tau_{\min}\lambda(t) < e_1 < \tau_{\max}\lambda(t), t > 0 \tag{40}$$

where $\tau_{\min}, \tau_{\max} > 0$ are the constant parameters.

Remark 3: From (39) and (40), the lower bound of undershoot and the upper bound of overshoot are limited by $-\tau_{\min}\lambda(0)$ while $\tau_{\max}\lambda(0)$, respectively. Besides, the transient performance of the system can be ensured by choosing the appropriate positive constants $\tau_{\min}, \tau_{\max}, \lambda_0, \lambda_\infty, \gamma$.

To apply the control design, a smooth and strictly increasing function $\mathbb{Q}(z)$ is recommended to convert the prescribed performance boundary into an equality form

$$\mathbb{Q}(z) = \frac{\tau_{\max}e^z - \tau_{\min}e^{-z}}{e^z + e^{-z}} \tag{41}$$

From (41), two conditions of $-\tau_{\min} < \mathbb{Q}(z) < \tau_{\max}$ and $\lim_{z\to\infty}\mathbb{Q}(z) = \tau_{\max}$, $\lim_{z\to-\infty}\mathbb{Q}(z) = -\tau_{\min}$ are satisfied. Hence, the constraint performance (40) can be rewritten

$$e_1 = \lambda(t)\mathbb{Q}(z) \tag{42}$$

Since $\mathbb{Q}(z)$ is a strictly monotonically increasing function and the initial condition is defined to satisfy $\lambda(t) > \lambda_\infty > 0$, we can receive the inverse transfer function $z = \mathbb{Q}^{-1}(e_1/\lambda(t))$.

Set $\phi = e_1/\lambda(t)$, we have the transform function of the intermediate variable $z(t)$

$$z(t) = \frac{1}{2}\ln\left(\frac{\phi + \tau_{\min}}{\tau_{\max} - \phi}\right) \tag{43}$$

Then, one defines the following state transformation

$$z_1 = z(t) - \frac{1}{2}\ln\frac{\tau_{\min}}{\tau_{\max}} \tag{44}$$

Lemma 4 [15]: On the basis of the above analysis, the convergence of the error signal e_1 can be ensured inside boundaries according to the prescribed performance constraint (40) under the transformation of the smooth function $\mathbb{Q}(z)$.

Remark 4: The control parameters $\lambda_0, \lambda_\infty, \gamma, \tau_{\min}, \tau_{\max}$ are selected for the control design. Since these parameters $\lambda_0, \tau_{\min}, \tau_{\max}$ satisfy the initial condition $-\tau_{\min}\lambda(0) < e_1(0) < \tau_{\max}\lambda(0)$, the new variable z_1 is kept within the boundaries and the inequality $-\tau_{\min} < \mathbb{Q}(z) < \tau_{\max}$ is maintained. The control problem is, therefore, guaranteed under the constraint $-\tau_{\min}\lambda(t) < e_1(t) < \tau_{\max}\lambda(t)$.

Step 2: Propose the intermediate control α_1.

The time derivative of z_1 is inferred from (43) by

$$\begin{aligned}\dot{z}_1 &= \frac{1}{2}\left(\frac{1}{\phi + \tau_{\min}} - \frac{1}{\phi - \tau_{\max}}\right)\left(\frac{\dot{x}_1}{\lambda} - \frac{x_1\dot{\lambda}}{\lambda^2}\right) \\ &= \beta\left(x_2 - \frac{x_1\dot{\lambda}}{\lambda}\right)\end{aligned} \tag{45}$$

where $\beta = \frac{1}{2\lambda}\left(\frac{1}{\phi+\tau_{\min}} - \frac{1}{\phi-\tau_{\max}}\right)$.

Define the error variable z_2

$$z_2 = \hat{x}_2 - \alpha_1 \tag{46}$$

The candidate Lyapunov function is chosen $V_1 = (1/2)\, z_1^2$, one can express the time derivative of V_1 as

$$\dot{V}_1 = z_1\dot{z}_1 \tag{47}$$

Based on the traditional backstepping, we get $\dot{V}_1$

$$\dot{V}_1 = z_1\beta\left(z_2 + \alpha_1 + \tilde{x}_2 - \frac{x_1\dot{\lambda}}{\lambda}\right) \tag{48}$$

Then, the virtual control α_1 is designed

$$\alpha_1 = -k_1\beta^{-1}z_1 + \frac{x_1\dot{\lambda}}{\lambda} \tag{49}$$

Substituting (49) into (48), we can rewrite $\dot{V}_1$ as follows

$$\dot{V}_1 = -k_1 z_1^2 + \beta z_1 z_2 + \beta z_1\tilde{x}_2 \tag{50}$$

Step 3: Propose the intermediate control α_2.

The command filtered technique is employed to design the controller in this step. Firstly, the tracking error e_2 is calculated by using the state observer variable

$$e_2 = \hat{x}_2 - x_2^c \tag{51}$$

where x_2^c represents the output signal of the virtual controller α_1.

The compensated tracking error is determined by

$$z_2 = e_2 - \mu_2 \tag{52}$$

The effect of command filtered error is diminished by the error compensation (21)

$$\dot{\mu}_2 = -k_2\mu_2 - g_2\mu_3 + g_2\left(x_3^c - \alpha_2\right) \tag{53}$$

where x_3^c denotes the output signal of the virtual controller α_2 which is defined in this step.

Using (12) and (29), we can express the time derivative of z_2

$$\begin{aligned}\dot{z}_2 = \theta_2^T S_2\left(\hat{\bar{x}}_2\right) + \tilde{\theta}_2^T S_2\left(\hat{\bar{x}}_2\right) + \upsilon_2 + a_2\tilde{x}_1 + e_3 + \alpha_2 - \dot{x}_2^c \\ + k_2\mu_2 - \mu_3\end{aligned} \tag{54}$$

where $\tilde{\theta}_2 = \theta_2^* - \theta_2$ is the estimation error.

Select the candidate Lyapunov function V_2

$$V_2 = V_1 + \frac{1}{2}z_2^2 + \frac{1}{2\varsigma_2}\upsilon_2^2 + \frac{1}{2\omega_2}\tilde{\theta}_2^T\tilde{\theta}_2 \tag{55}$$

Taking the derivative of V_2 using (54) we have

$$\begin{aligned}\dot{V}_2 = -k_1 z_1^2 + z_2\left(\beta z_1 + \dot{z}_2\right) + \varsigma_2^{-1}\upsilon_2\dot{\upsilon}_2 \\ - \omega_2^{-1}\tilde{\theta}_2^T\dot{\theta}_2 + \beta z_1\tilde{x}_2\end{aligned} \tag{56}$$

Using (51), (52), and (53), we can write (56) as follows

$$\begin{aligned}\dot{V}_2 &= -k_1 z_1^2 \\ &\quad + z_2\left(\begin{array}{c}\beta z_1 + \theta_2^T S_2\left(\hat{\bar{x}}_2\right) + \tilde{\theta}_2^T S_2\left(\hat{\bar{x}}_2\right) + \upsilon_2 + a_2\tilde{x}_1 \\ + e_3 + \alpha_2 - \dot{x}_2^c + k_2\mu_2 - \mu_3\end{array}\right) \\ &\quad + \varsigma_2^{-1}\upsilon_2\dot{\upsilon}_2 - \omega_2^{-1}\tilde{\theta}_2^T\dot{\theta}_2 + \beta z_1\tilde{x}_2\end{aligned} \tag{57}$$

Choose the virtual control α_2

$$\alpha_2 = -\beta z_1 - \theta_2^T S_2\left(\hat{\bar{x}}_2\right) - k_2 e_2 - a_2\tilde{x}_1 + \dot{x}_2^c \tag{58}$$

Besides, the adaptive law is proposed as

$$\dot{\theta}_2 = \omega_2\left(\left(z_2 + \frac{\upsilon_2}{\varsigma_2}\right)S_2\left(\hat{\bar{x}}_2\right) - \xi_2\theta_2\right) \tag{59}$$

where $\omega_2 > 0$, $\varsigma_2 > 0$, and $\xi_2 > 0$ are design parameters.

From (37), we can write

$$\dot{\upsilon}_2 = \tilde{\theta}_2^T S_2\left(\hat{\bar{x}}_2\right) + a_2\tilde{x}_1 - \varpi_2\upsilon_2 - \tilde{\theta}_2^T S_2\left(\hat{\bar{x}}_2\right) \tag{60}$$

Using (58) and (59), we can write (57) based on Young's inequality

$$\begin{aligned}\dot{V}_2 &= -k_1 z_1^2 - \left(k_2 - \frac{1}{2}\right)z_2^2 + z_2 z_3 + \frac{1}{2}\upsilon_2^{*2} \\ &\quad + \xi_2\tilde{\theta}_2^T\theta_2 + \beta z_1\tilde{x}_2 \\ &\quad + \varsigma_2^{-1}\upsilon_2\left(a_2\tilde{x}_1 - \varpi_2\upsilon_2 - \tilde{\theta}_2^T S_2\left(\hat{\bar{x}}_2\right)\right)\end{aligned} \tag{61}$$

Step 4: Design the actual control u_d^s.

The tracking error e_3 can be defined similarly to step 3

$$e_3 = \hat{x}_5 - x_3^c \tag{62}$$

Then, the compensated tracking error is defined

$$z_3 = e_3 - \mu_3 \tag{63}$$

From (21), the compensating signal is used

$$\dot{\mu}_3 = -k_3\mu_3 - g_2\mu_2 \tag{64}$$

Using (29) and (62), we can acquire the time derivative of z_3 (63) by

$$\begin{aligned} \dot{z}_3 &= \dot{e}_3 - \dot{\varphi}_3 \\ &= \left(\theta_G^{*T} S_G\left(\hat{\bar{x}}_1\right) + \upsilon_G\right) u_d^s + \theta_3^{*T} S_3\left(\hat{\bar{x}}_3\right) + \upsilon_3 \\ &\quad + a_3\left(x_1 - \hat{x}_1\right) - \dot{x}_3^c + k_3\mu_3 + \mu_2 \end{aligned} \tag{65}$$

where $\tilde{\theta}_3 = \theta_3^* - \theta_3$ and $\tilde{\theta}_G = \theta_G^* - \theta_G$ are estimation errors.
The candidate Lyapunov function V_3 is selected by

$$V_3 = V_2 + \frac{1}{2}z_3^2 + \frac{1}{2\varsigma_3}\nu_3^2 + \frac{1}{2\omega_3}\tilde{\theta}_3^T\tilde{\theta}_3 + \frac{1}{2\omega_G}\tilde{\theta}_G^T\tilde{\theta}_G \tag{66}$$

Then, the time derivative of V_3 using (61) can be expressed

$$\begin{aligned} \dot{V}_3 &= -k_1 z_1^2 - \left(k_2 - \frac{1}{2}\right) z_2^2 + \frac{1}{2}\upsilon_2^{*2} + \xi_2\tilde{\theta}_2^T\theta_2 + z_2 z_3 \\ &\quad + \beta z_1\tilde{x}_2 + z_3\dot{z}_3 + \varsigma_3^{-1}\nu_3\dot{\nu}_3 + \omega_3^{-1}\tilde{\theta}_3^T\dot{\tilde{\theta}}_3 + \omega_G^{-1}\tilde{\theta}_G^T\dot{\tilde{\theta}}_G \\ &\quad + \varsigma_2^{-1}\nu_2\left(a_2\tilde{x}_1 - \varpi_2\nu_2 - \tilde{\theta}_2^T S_2\left(\hat{\bar{x}}_2\right)\right) \end{aligned} \tag{67}$$

Substituting (65) into (67), we obtain

$$\begin{aligned} \dot{V}_3 &= -k_1 z_1^2 - \left(k_2 - \frac{1}{2}\right) z_2^2 + \frac{1}{2}\upsilon_2^{*2} + \xi_2\tilde{\theta}_2^T\theta_2 + z_2 z_3 \\ &\quad + \beta z_1\tilde{x}_2 + \varsigma_3^{-1}\nu_3\dot{\nu}_3 - \omega_3^{-1}\tilde{\theta}_3^T\dot{\theta}_3 - \omega_G^{-1}\tilde{\theta}_G^T\dot{\theta}_G \\ &\quad + \varsigma_2^{-1}\nu_2\left(a_2\tilde{x}_1 - \varpi_2\nu_2 - \tilde{\theta}_2^T S_2\left(\hat{\bar{x}}_2\right)\right) \\ &\quad + z_3\left(\begin{array}{c}\left(\theta_G^{*T} S_G\left(\hat{\bar{x}}_1\right) + \upsilon_G\right) u_d^s + \theta_3^{*T} S_3\left(\hat{\bar{x}}_3\right) + \upsilon_3 \\ + a_3\left(x_1 - \hat{x}_1\right) - \dot{x}_3^c + k_3\mu_3 + \mu_2\end{array}\right) \end{aligned} \tag{68}$$

Propose the actual control u_d^s

$$u_d^s = \left[\theta_G^T S_G\left(\hat{\bar{x}}_1\right)\right]^{-1}\left(-\theta_3^T S_3\left(\hat{\bar{x}}_3\right) - a_3\tilde{x}_1 + \dot{x}_3^c - k_3 e_3 - e_2\right) \tag{69}$$

Substituting (69) into (68), we have

$$\begin{aligned} \dot{V}_3 &= -k_1 z_1^2 - \left(k_2 - \frac{1}{2}\right) z_2^2 + \frac{1}{2}\upsilon_2^{*2} + \xi_2\tilde{\theta}_2^T\theta_2 + z_2 z_3 \\ &\quad + \beta z_1\tilde{x}_2 + \varsigma_3^{-1}\nu_3\dot{\nu}_3 - \omega_3^{-1}\tilde{\theta}_3^T\dot{\theta}_3 - \omega_G^{-1}\tilde{\theta}_G^T\dot{\theta}_G \\ &\quad + \varsigma_2^{-1}\nu_2\left(a_2\tilde{x}_1 - \varpi_2\nu_2 - \tilde{\theta}_2^T S_2\left(\hat{\bar{x}}_2\right)\right) \\ &\quad + z_3\left(\begin{array}{c}\left(\tilde{\theta}_G^T S_G\left(\hat{\bar{x}}_1\right) + \upsilon_G\right) u_d^s + \tilde{\theta}_3^T S_3\left(\hat{\bar{x}}_3\right) + \upsilon_3 \\ -k_3 z_3 - z_2\end{array}\right) \end{aligned} \tag{70}$$

The adaptive law is proposed as

$$\begin{aligned} \dot{\theta}_3 &= \omega_3\left(\left(z_3 + \frac{\nu_3}{\varsigma_3}\right) S_3\left(\hat{\bar{x}}_3\right) - \xi_3\theta_3\right) \qquad (71) \\ \dot{\theta}_G &= \omega_G\left(z_3 u_d^s S_G\left(\hat{\bar{x}}_1\right) - \xi_G\theta_G\right) \qquad (72) \end{aligned}$$

where $\omega_3, \omega_G, \xi_3, \xi_G, \varsigma_3$ are design parameters.
From (37), we can obtain

$$\dot{\nu}_3 = \tilde{\theta}_3^T S_3\left(\hat{\bar{x}}_3\right) + a_3\tilde{x}_1 - \varpi_3\nu_3 - \tilde{\theta}_3^T S_3\left(\hat{\bar{x}}_3\right) \tag{73}$$

Assume that the control signal u_d^s is bounded $\left|u_d^s\right| \le u_d^*$, apply Young's inequality theory, we receive

$$\begin{aligned} z_3\upsilon_G u_d^s &\le \frac{1}{2}z_3^2 + \frac{1}{2}\upsilon_G^{*2}u_d^{*2} \\ z_3\upsilon_3 &\le \frac{1}{2}z_3^2 + \frac{1}{2}\upsilon_3^{*2} \end{aligned} \tag{74}$$

Substituting (71), (72), (73), and (74) into (70), we can write

$$\begin{aligned} \dot{V}_3 &= -k_1 z_1^2 - \left(k_2 - \frac{1}{2}\right) z_2^2 - \left(k_3 - 1\right) z_3^2 + \xi_2\tilde{\theta}_2^T\theta_2 + \beta z_1\tilde{x}_2 \\ &\quad + \xi_3\tilde{\theta}_3^T\theta_3 + \xi_G\tilde{\theta}_G^T\theta_G + \frac{1}{2}\upsilon_2^{*2} + \frac{1}{2}\upsilon_3^{*2} + \frac{1}{2}\upsilon_G^{*2}u_d^{*2} \\ &\quad + \varsigma_2^{-1}\nu_2\left(a_2\tilde{x}_1 - \varpi_2\nu_2 - \tilde{\theta}_2^T S_2\left(\hat{\bar{x}}_2\right)\right) \\ &\quad + \varsigma_3^{-1}\nu_3\left(a_3\tilde{x}_1 - \varpi_3\nu_3 - \tilde{\theta}_3^T S_3\left(\hat{\bar{x}}_3\right)\right) \end{aligned} \tag{75}$$

Theorem: Considering the pneumatic active suspension with actuator characteristics (4) and (7) under Assumptions 1 - 3, virtual control (49), (58), actual control (69), and the fuzzy serial-parallel observer (29), (35) are designed. Based on the proposed method, the tracking errors and scaled state estimation errors $\tilde{x}_i$ are guaranteed to be bounded. Then, all system signals are semi-global uniformly ultimately bounded. By choosing proper control parameters, the tracking error e_1 converges to the boundary of the PPF constraints.

Proof: Define a general candidate Lyapunov function V considering the observer estimation error

$$V = V_3 + \frac{1}{2}\tilde{x}^T P\tilde{x} \tag{76}$$

where P is the positive symmetric matrix such that $A^T P + PA = -Q$.
Using (70), we obtain the time derivative of V by

$$\begin{aligned} \dot{V} &= -k_1 z_1^2 - \left(k_2 - \frac{1}{2}\right) z_2^2 - \left(k_3 - 1\right) z_3^2 + \xi_2\tilde{\theta}_2^T\theta_2 + \beta z_1\tilde{x}_2 \\ &\quad + \xi_3\tilde{\theta}_3^T\theta_3 + \xi_G\tilde{\theta}_G^T\theta_G + \frac{1}{2}\upsilon_2^{*2} + \frac{1}{2}\upsilon_3^{*2} + \frac{1}{2}\upsilon_G^{*2}u_d^{*2} \\ &\quad + \varsigma_2^{-1}\nu_2\left(a_2\tilde{x}_1 - \varpi_2\nu_2 - \tilde{\theta}_2^T S_2\left(\hat{\bar{x}}_2\right)\right) \\ &\quad + \varsigma_3^{-1}\nu_3\left(a_3\tilde{x}_1 - \varpi_3\nu_3 - \tilde{\theta}_3^T S_3\left(\hat{\bar{x}}_3\right)\right) \\ &\quad + \frac{1}{2}\dot{\tilde{x}}^T P\tilde{x} + \frac{1}{2}\tilde{x}^T P\dot{\tilde{x}} \end{aligned} \tag{77}$$

Set $\delta = [\delta_1, \delta_2, \delta_3]^T$, then substitute (31) into (77), we have:

$$\begin{aligned}\dot{V} &= -k_1 z_1^2 - \left(k_2 - \frac{1}{2}\right) z_2^2 - (k_3 - 1) z_3^2 + \xi_2 \tilde{\theta}_2^T \theta_2 + \beta z_1 \tilde{x}_2 \\ &\quad + \xi_3 \tilde{\theta}_3^T \theta_3 + \xi_G \tilde{\theta}_G^T \theta_G + \frac{1}{2}\upsilon_2^{*2} + \frac{1}{2}\upsilon_3^{*2} + \frac{1}{2}\upsilon_G^{*2} u_d^{*2} \\ &\quad + \varsigma_2^{-1} \nu_2 \left(a_2 \tilde{x}_1 - \varpi_2 \nu_2 - \tilde{\theta}_2^T S_2\left(\hat{\bar{x}}_2\right)\right) \\ &\quad + \varsigma_3^{-1} \nu_3 \left(a_3 \tilde{x}_1 - \varpi_3 \nu_3 - \tilde{\theta}_3^T S_3\left(\hat{\bar{x}}_3\right)\right) \\ &\quad + \frac{1}{2}\tilde{x}^T \left(A^T P + PA\right) \tilde{x} + \tilde{x}^T P \left(\delta + B_3 \delta_G u_d^s + D\right) \qquad (78)\end{aligned}$$

Based on (33), (34) and Young's inequality, we have

$$\begin{aligned}&\tilde{x}^T P \delta \\ &\le \frac{\upsilon \|P\|^2 \|\tilde{x}\|^2}{2} + \frac{\sum_{i=1}^3 \left\|\theta_i^*\right\|^2 S_i^T(\bar{x}_i) S_i(\bar{x}_i)}{2\upsilon} \\ &\quad + \frac{\upsilon \|P\|^2 \|\tilde{x}\|^2}{2} \\ &\quad + \frac{\sum_{i=1}^3 \left\|\theta_i^*\right\|^2 S_i^T\left(\hat{\bar{x}}_i\right) S_i\left(\hat{\bar{x}}_i\right)}{2\upsilon} + \frac{\upsilon \|P\|^2 \|\tilde{x}\|^2}{2} \\ &\quad + \frac{\sum_{i=1}^3 \left\|\tilde{\theta}_i\right\|^2 S_i^T\left(\hat{\bar{x}}_i\right) S_i\left(\hat{\bar{x}}_i\right)}{2\upsilon} + \frac{\upsilon \|P\|^2 \|\tilde{x}\|^2}{2} \\ &\quad + \frac{\sum_{i=1}^3 \varepsilon_i^{*2}}{2\upsilon} \\ &\le 2\upsilon \|P\|^2 \|\tilde{x}\|^2 + \sum_{i=1}^3 \left[\frac{\left\|\theta_i^*\right\|^2}{\upsilon} + \frac{\left\|\tilde{\theta}_i\right\|^2}{2\upsilon} + \frac{\varepsilon_i^{*2}}{2\upsilon}\right]\end{aligned}$$

$$\begin{aligned}&\tilde{x}^T P B_3 \delta_G u_d^s \\ &\le \frac{\upsilon \|P\|^2 \|\tilde{x}\|^2}{2} + \frac{\left\|\theta_G^*\right\|^2 S_G^T(\bar{x}_1) S_i(\bar{x}_1)}{2\upsilon} u^2 \\ &\quad + \frac{\upsilon \|P\|^2 \|\tilde{x}\|^2}{2} + \frac{\left\|\theta_G^*\right\|^2 S_G^T\left(\hat{\bar{x}}_1\right) S_G\left(\hat{\bar{x}}_1\right)}{2\upsilon} u_d^{*2} \\ &\quad + \frac{\upsilon \|P\|^2 \|\tilde{x}\|^2}{2} \\ &\quad + \frac{\left\|\tilde{\theta}_G\right\|^2 S_G^T\left(\hat{\bar{x}}_1\right) S_G\left(\hat{\bar{x}}_1\right)}{2\upsilon} u_d^{*2} + \frac{\upsilon \|P\|^2 \|\tilde{x}\|^2}{2} + \frac{\varepsilon_G^{*2}}{2\upsilon} u_d^{*2} \\ &\le 2\upsilon \|P\|^2 \|\tilde{x}\|^2 + \frac{\left\|\tilde{\theta}_G\right\|^2}{2\upsilon} u_d^{*2} + \left(\frac{\left\|\theta_G^*\right\|^2}{\upsilon} + \frac{\varepsilon_G^{*2}}{2\upsilon}\right) u_d^{*2}\end{aligned}$$

$$\begin{aligned}&\tilde{x}^T P D \\ &\le \frac{1}{2}\|\tilde{x}\|^2 + \frac{1}{2}\|P\|^2 \sum_{i=1}^3 \bar{d}_i^2\end{aligned}$$

where υ is a positive constant and the FLSs theory proved that $0 < S_i^T(.) S_i(.) \le 1$. Assume that the disturbances are bounded by $|d_1| \le \bar{d}_i$, $i = 1, 2, 3$.

Similarly, the following inequality can be obtained

$$\begin{aligned}\beta z_1 \tilde{x}_2 &\le \frac{1}{2}\beta^2 z_1^2 + \frac{1}{2}\|\tilde{x}\|^2 \\ \nu_2 a_2 \tilde{x}_1 &\le \frac{\nu_2^2 a_2^2}{4} + \|\tilde{x}\|^2 \\ \nu_3 a_3 \tilde{x}_1 &\le \frac{\nu_3^2 a_3^2}{4} + \|\tilde{x}\|^2 \\ -\nu_2 \tilde{\theta}_2^T S_2\left(\hat{\bar{x}}_2\right) &\le \frac{\nu_2^2}{4} + \tilde{\theta}_2^T \tilde{\theta}_2 \\ -\nu_3 \tilde{\theta}_3^T S_3\left(\hat{\bar{x}}_3\right) &\le \frac{\nu_3^2}{4} + \tilde{\theta}_3^T \tilde{\theta}_3 \\ \xi_2 \tilde{\theta}_2^T \theta_2 &\le \frac{\xi_2}{2}\left\|\theta_2^*\right\|^2 - \frac{\xi_2}{2}\left\|\tilde{\theta}_2\right\|^2 \\ \xi_3 \tilde{\theta}_3^T \theta_3 &\le \frac{\xi_3}{2}\left\|\theta_3^*\right\|^2 - \frac{\xi_3}{2}\left\|\tilde{\theta}_3\right\|^2 \\ \xi_G \tilde{\theta}_G^T \theta_G &\le \frac{\xi_G}{2}\left\|\theta_G^*\right\|^2 - \frac{\xi_G}{2}\left\|\tilde{\theta}_G\right\|^2\end{aligned}$$

Thus, we can further write (78) as follows

$$\begin{aligned}\dot{V} &\le -\left(k_1 - \frac{1}{2}\beta^2\right) z_1^2 - \left(k_2 - \frac{1}{2}\right) z_2^2 - (k_3 - 1) z_3^2 \\ &\quad - \varsigma_2^{-1}\left(\frac{a_2^2}{4} + \varpi_2 - \frac{1}{4}\right)\nu_2^2 - \varsigma_3^{-1}\left(\frac{a_3^2}{4} + \varpi_3 - \frac{1}{4}\right)\nu_3^2 \\ &\quad - \left(\frac{\xi_2}{2} - \varsigma_2^{-1} - \frac{1}{2\upsilon}\right)\left\|\tilde{\theta}_2\right\|^2 - \left(\frac{\xi_3}{2} - \varsigma_3^{-1} - \frac{1}{2\upsilon}\right)\left\|\tilde{\theta}_3\right\|^2 \\ &\quad - \left(\frac{\xi_G}{2} - \frac{u_d^{*2}}{2\upsilon}\right)\left\|\tilde{\theta}_G\right\|^2 \\ &\quad - \left(\lambda_{\min}(Q) - \varsigma_2^{-1} - \varsigma_3^{-1} - 4\upsilon\|P\|^2 - 1\right)\|\tilde{x}\|^2 \\ &\quad + \frac{\xi_2}{2}\left\|\theta_2^*\right\|^2 + \frac{\xi_3}{2}\left\|\theta_3^*\right\|^2 + \frac{\xi_G}{2}\left\|\theta_G^*\right\|^2 + \frac{1}{2}\upsilon_2^{*2} + \frac{1}{2}\upsilon_3^{*2} \\ &\quad + \left(\frac{\left\|\theta_G^*\right\|^2}{\upsilon} + \frac{\varepsilon_G^{*2}}{2\upsilon} + \frac{1}{2}\upsilon_G^{*2}\right) u_d^{*2} + \sum_{i=1}^3\left(\frac{\left\|\theta_i^*\right\|^2}{\upsilon} + \frac{\varepsilon_i^{*2}}{2\upsilon}\right) \\ &\quad + \frac{1}{2}\|P\|^2 \sum_{i=1}^3 \bar{d}_i^2 \qquad (79)\end{aligned}$$

Define

$$\begin{aligned}\Psi &= \frac{\xi_2}{2}\left\|\theta_2^*\right\|^2 + \frac{\xi_3}{2}\left\|\theta_3^*\right\|^2 + \frac{\xi_G}{2}\left\|\theta_G^*\right\|^2 + \frac{1}{2}\upsilon_2^{*2} \\ &\quad + \frac{1}{2}\|P\|^2 \sum_{i=1}^3 \bar{d}_i^2 \\ &\quad + \frac{1}{2}\upsilon_3^{*2} + \left(\frac{\left\|\theta_G^*\right\|^2}{\upsilon} + \frac{\varepsilon_G^{*2}}{2\upsilon}\frac{1}{2}\upsilon_G^{*2}\right) u_d^{*2} \\ &\quad + \sum_{i=1}^3\left(\frac{\left\|\theta_i^*\right\|^2}{\upsilon} + \frac{\varepsilon_i^{*2}}{2\upsilon}\right)\end{aligned}$$

$$\begin{aligned}\Omega &= min \\ &\cdot\left\{\begin{array}{l} 2\left(k_1 - \frac{1}{2}\beta^2\right); 2\left(k_2 - \frac{1}{2}\right); 2(k_3 - 1); \varsigma_2^{-1}\left(\frac{a_2^2}{4} + \varpi_2 - \frac{1}{4}\right) \\ \varsigma_3^{-1}\left(\frac{a_3^2}{4} + \varpi_3 - \frac{1}{4}\right); 2\left(\frac{\xi_2}{2} - \varsigma_2^{-1} - \frac{1}{2\upsilon}\right); \left(\frac{\xi_3}{2} - \varsigma_3^{-1} - \frac{1}{2\upsilon}\right) \\ 2\left(\frac{\xi_G}{2} - \frac{u_d^{*2}}{2\upsilon}\right); 2\left(\lambda_{\min}(Q) - \varsigma_2^{-1} - \varsigma_3^{-1} - 4\upsilon\|P\|^2 - 1\right) \end{array}\right\}\end{aligned}$$

Then we can simplify (79) as follows

$$\dot{V} \le -\Omega V + \Psi \qquad (80)$$

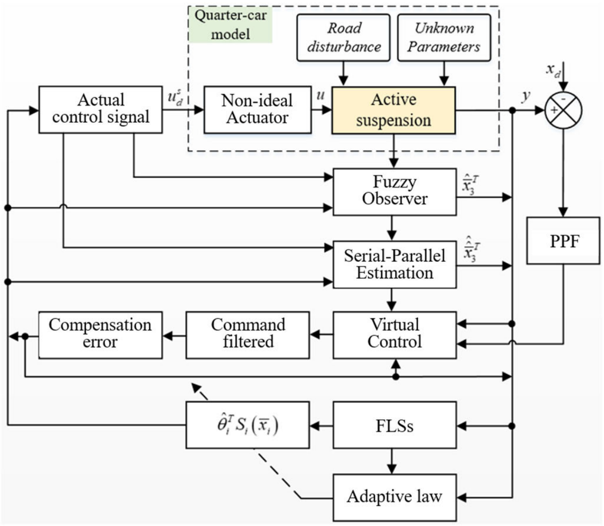

FIGURE 2. Block diagram of the proposed control structure.

Multiplying (80) by $e^{\Omega t}$ on both sides and integrating, we get

$$\int_0^t \left(e^{\Omega t} V\right)' dt \le \Psi \int_0^t e^{\Omega t} dt \tag{81}$$

$$\begin{aligned} V(t) &\le \left(V(0) - \frac{\Psi}{\Omega}\right) e^{-\Omega t} + \frac{\Psi}{\Omega} \\ &\le V(0)\, e^{-\Omega t} + \frac{\Psi}{\Omega} \end{aligned} \tag{82}$$

Hence, the following conditions can be proved from (76)

$$|z_i| \le \sqrt{2\left(V(0)\, e^{-\Omega t} + \frac{\Psi}{\Omega}\right)}, \quad i = 1, 2, 3 \tag{83}$$

Based on the above results, we can conclude that transformation errors $z_i, i = 1, 2, 3$ and compensated signals $\mu_i, i = 1, 2, 3$ are bounded, resulting in the tracking errors e_1, e_2, e_3 are also bounded. Therefore, the stability of the closed-loop system is proved by choosing the design parameters.

Remark 5: Since the estimation tracking errors $\tilde{x}_i, \tilde{\theta}_i, i = 2, 3$, and $\tilde{\theta}_G$ are bounded according to (82), their estimation values are also bounded in a finite time by selecting control gains. Thus, the proposed control scheme can approximate unmeasured states to guarantee the suspension performance under the influence of unknown parameters.

The block diagram of the proposed control can be illustrated in Fig. 2.

C. HANDLING STABILITY AND ROAD HOLDING ANALYSIS

From the above analysis, the developed control method has satisfied the main objective of passenger comfort. However, improving the ride comfort will enhance suspension deflection. Besides, it also contradicts the objective of ensuring tire contact with the road profile. Therefore, in this section, two objectives of handling stability and road holding are ensured by selecting proper design parameters. To analyze these objectives, we concentrate on unsprung mass mechanical equations of the pneumatic suspension (11). Besides, the tracking errors e_1, e_2, e_3 are proved to be bounded based on the result (83). Using the FLSs approximation for $f_2 = \theta_2 S_2(X_2) + \eta_2(X_2)$, we get

$$\dot{X} = EX + FY + X_0 \tag{84}$$

where

$$X = \begin{bmatrix} x_3 \\ x_4 \end{bmatrix}; \quad E = \begin{bmatrix} 0 & 1 \\ -\dfrac{k_{st}}{m_u} & -\dfrac{c_{at}}{m_u} \end{bmatrix};$$

$$F = \begin{bmatrix} 0 & 0 \\ \dfrac{k_{st}}{m_u} & \dfrac{c_{at}}{m_u} \end{bmatrix}; \quad Y = \begin{bmatrix} z_r \\ \dot{z}_r \end{bmatrix}$$

$$X_0 = \begin{bmatrix} 0 \\ Z \end{bmatrix};$$

$$Z = \frac{m_s}{m_u}\left(\theta_2^T S_2(X_2) + \eta_2(X_2)\right) - \frac{1}{m_u}(m_s x_5 + m_s x_2)$$

Based on (83), the unknown term Z is bounded because the tracking errors z_1, z_2, and z_3 are bounded with the proposed control. There exists a constant $\bar{Z}$ so that $\|Z\| \le \bar{Z}$ is satisfied.

Choose the candidate Lyapunov function

$$V_A = X^T P X \tag{85}$$

where P is a positive definite symmetric matrix.

Then, we can obtain the time derivative of V_A by

$$\dot{V}_A = \dot{X}^T P X + X^T P \dot{X} \tag{86}$$

Rewrite (86) using (84), we receive

$$\dot{V}_A = X^T\left(E^T P + PE\right) X + 2X^T PFY + 2X^T PX_0 \tag{87}$$

There exists a positive definite symmetric matrix $Q > 0$ so that the equation $E^T P + PE = -Q$ is satisfied. Besides, according to Young's inequality theorem, the form of $2X^T PFY$ and $2X^T PX_0$ can be expressed by

$$\begin{aligned} 2X^T PFY &\le \frac{1}{\pi_1} X^T PFF^T PX + \pi_1 Y^T Y \\ 2X^T PX_0 &\le \frac{1}{\pi_2} X^T PPX + \pi_2 X_0^T X_{.0} \end{aligned} \tag{88}$$

where $\pi_i > 0, i = 1, 2$ are the design parameters.

Substituting (88) into (87), one obtains

$$\begin{aligned} \dot{V}_A \le -&\begin{bmatrix} \lambda_{\min}\left(P^{-1/2} Q P^{-1/2}\right) - \dfrac{1}{\pi_1}\lambda_{\max}\left(P^{1/2} FF^T P^{1/2}\right) \\ -\dfrac{1}{\pi_2}\lambda_{\max}(P) \end{bmatrix} V_A \\ &+ \pi_1 Y^T Y + \pi_2 X_0^T X_0 \end{aligned} \tag{89}$$

where $\lambda_{\max}, \lambda_{\min}$ are the maximal and minimal eigenvalues.

For the control design, the appropriate matrix P, Q can be selected to satisfy the following inequalities

$$\pi_1 > 2\frac{\lambda_{\max}\left(P^{1/2} FF^T P^{1/2}\right)}{\lambda_{\min}\left(P^{-1/2} Q P^{-1/2}\right)} \text{ and } \pi_2 > 2\frac{\lambda_{\max}(P)}{\lambda_{\min}\left(P^{-1/2} Q P^{-1/2}\right)} \tag{90}$$

We can define Θ and Υ satisfying the condition at (90)

$$\Theta \geq \lambda_{\min}\left(P^{-1/2}QP^{-1/2}\right) - \frac{1}{\pi_1}\lambda_{\max}\left(P^{1/2}FF^TP^{1/2}\right) - \frac{1}{\pi_2}\lambda_{\max}(P) \quad (91)$$

$$\Upsilon \geq \pi_1 Y^T Y + \pi_2 X_0^T X_0 \quad (92)$$

Therefore, we can express the inequality (89) as follows

$$\dot{V}_A \leq -\Theta V_A + \Upsilon \quad (93)$$

Multiplying (93) by $e^{\Theta t}$ on both sides and integrating

$$V_A \leq \left(V_A(0) - \frac{\Upsilon}{\Theta}\right)e^{-\Theta t} + \frac{\Upsilon}{\Theta} \leq V_A(0)\,e^{-\Theta t} + \frac{\Upsilon}{\Theta} \quad (94)$$

According to (85), the system states (11) are bounded by

$$|x_i(t)| \leq \sqrt{\left(V_A(0)\,e^{-\Theta t} + \frac{\Upsilon}{\Theta}\right)/\lambda_{\min}(P)}, \quad i = 3, 4 \quad (95)$$

Substituting (95) into the handling stability condition (23)

$$|z_s - z_s| = |x_1 - x_3| \leq |x_1| + |x_3| \leq \tau_{\max}\lambda(0) + \sqrt{\left(V_A(0)\,e^{-\Theta t} + \frac{\Upsilon}{\Theta}\right)/\lambda_{\min}(P)} \quad (96)$$

From (96), the handling stability condition is guaranteed by choosing control parameters π_1, π_2, P, and appropriate PPF constraints $\tau_{\max}, \tau_{\min}, \lambda(0)$ so that $|z_s - z_s| \leq z_M$.

Besides, the tire forces F_{st} and F_{at} can be expressed by (95)

$$\begin{aligned} F_{st}(z_u, z_r, t) &= k_{st}(x_3 - z_r) \\ &\leq k_{st}\sqrt{\left(V_A(0)\,e^{-\Theta t} + \frac{\Upsilon}{\Theta}\right)/\lambda_{\min}(P)} + k_{st}\|z_r\|_\infty \\ F_{at}(z_u, z_r, t) &= c_{at}(x_4 - \dot{z}_r) \\ &\leq c_{at}\sqrt{\left(V_A(0)\,e^{-\Theta t} + \frac{\Upsilon}{\Theta}\right)/\lambda_{\min}(P)} + c_{at}\|\dot{z}_r\|_\infty \end{aligned} \quad (97)$$

Based on (97) into, we write the relative tire force by

$$\begin{aligned} |F_{tr}| &\leq |F_{st}| + |F_{at}| \\ &\leq (k_{st} + c_{at})\sqrt{\left(V_A(0)\,e^{-\Theta t} + \frac{\Upsilon}{\Theta}\right)/\lambda_{\min}(P)} \\ &\quad + k_{st}\|z_r\|_\infty + c_{at}\|\dot{z}_r\|_\infty \end{aligned} \quad (98)$$

Based on (98), choosing appropriate design parameters π_1, π_2, P which meet the inequality $|F_{st} + F_{at}| \leq (m_s + m_u)\,g$, the relative tire force condition (24) could be guaranteed.

Remark 6: From the above results, the suspension objectives of handling stability and road holding can be archived by selecting appropriate initial conditions and control parameters. Hence, the pneumatic suspension works properly under the requirement of mechanical structure and driving safety.

TABLE 1. Pneumatic active suspension parameters.

Parameter	Value	Unit	Parameter	Value	Unit
m_s	$550 \pm 100\sin(\pi t)$	kg	z_M	0.04	m
m_u	60	kg	z_{as0}	0.18	m
k_s	18000	Nm^{-1}	R	287.5	J/kgK
k_{st}	145000	Nm^{-1}	A_{as}	0.0047	m^2
c_a	2600	Nsm^{-1}	κ	1.4	-
c_{at}	1200	Nsm^{-1}	T	293.15	K

TABLE 2. Control parameters.

Controller	Parameter
Backstepping	$k_1 = 30, k_2 = 40, k_3 = 20$
Back-CFC	$k_1 = 30, k_2 = 40, k_3 = 20, \rho_m = 300, o_m = 0$
Back-PPF	$k_1 = 30, k_2 = 40, k_3 = 20$
	$\lambda_0 = 0.058, \lambda_\infty = 0.0058, \gamma = 2.2$
Proposed	$k_1 = 30, k_2 = 40, k_3 = 20$
	$a_1 = 10, a_2 = 20, a_3 = 40, \rho_m = 300$
	$\varpi_1 = 5, \varpi_2 = 5, \varpi_3 = 5, o_m = 0.5$
	$\varsigma_2 = 0.3, \varsigma_3 = 0.2, \varsigma_G = 0.6$
	$\omega_2 = 0.5, \omega_3 = 0.4, \omega_G = 0.3$

IV. SIMULATION RESULTS AND DISCUSSION

A. SIMULATION DESCRIPTION

To demonstrate the effectiveness of the control scheme, the comparative simulation examples are compared with passive suspension, traditional backstepping, CFC backstepping (Back-CFC), and PPF backstepping (Back-PPF). Besides, the root mean square (RMS) values of chassis acceleration are considered to evaluate passenger comfort, which is dependent on the human body's sensitivity to acceleration. Finally, two objectives of handling stability and road holding are analyzed by considering RSD and RTF parameters. The main parameters of the pneumatic suspension are given in Table 1.

The sinusoidal function with an amplitude of 0.02 m and frequency of 1 Hz is applied to simulate the road excitation $z_r = 0.02\sin(2\pi t)$.The initial values of the system states are selected by $x_1(0) = 0.05$, $x_2(0) = x_3(0) = x_4(0) = 0$, and $x_5(0) = 1.0 \times 10^5$ (Pa). The prescribed performance constraints are chosen by $\lambda_0 = 0.058$, $\lambda_\infty = 0.0058$, $\gamma = 2.2$ and design parameters $\tau_{\min} = 0.98$, $\tau_{\max} = 0.98$.The detailed control parameters are compared in Table 2.

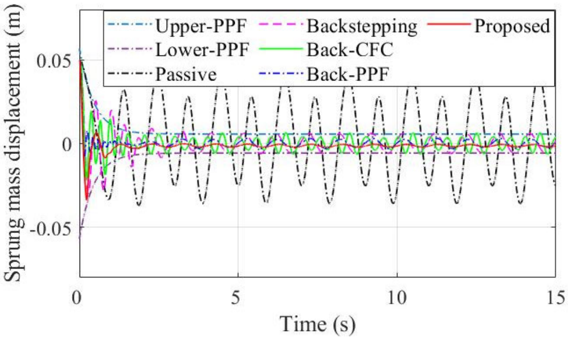

FIGURE 3. Simulation result of sprung mass displacement.

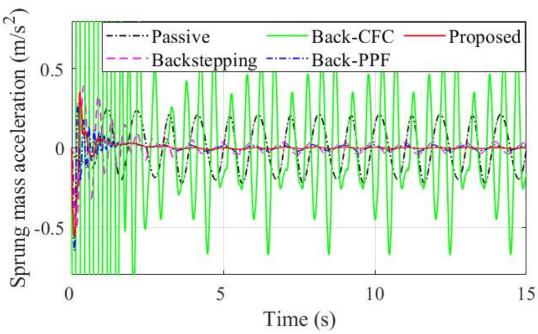

FIGURE 4. Simulation result of sprung mass acceleration.

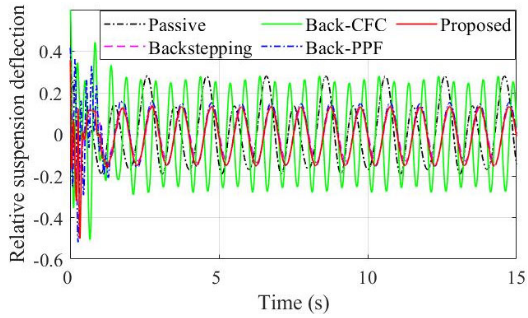

FIGURE 5. Relative suspension deflection.

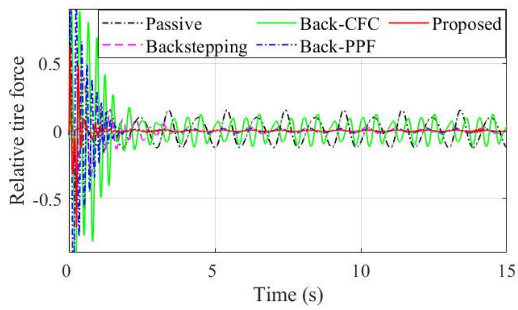

FIGURE 6. Relative tire force.

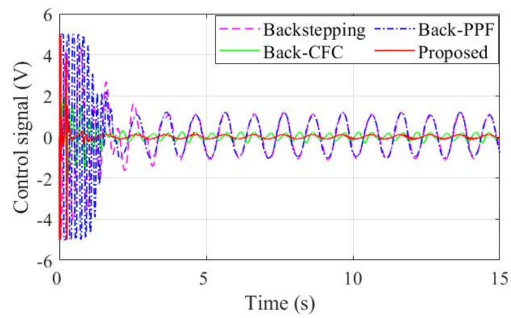

FIGURE 7. Control signal (V).

B. SIMULATION RESULTS

Figs. 3 - 7 display the simulation results of sprung mass acceleration and displacement, relative suspension deflection, relative tire force, and input control signals of passive, traditional backstepping, Back-CFC, Back-PPF, and proposed control. Results show that the developed method can minimize sprung mass vibration from road excitation to maximize passenger comfort. By employing the PPF constraint, the developed scheme can provide the best vibration dissipation since it can limit the convergence of the tracking error inside the boundary constraints as shown in Fig. 3. Besides, chassis displacement can achieve the fasted convergence to zero at a time $t = 2.0$ (s). Although back-PPF can provide the ability to ensure the tracking error inside the boundaries, the sprung mass displacement cannot be forced to zero position. Under the effects of unknown parameters and a non-ideal actuator, traditional backstepping can provide the normal suspension performance while the back-CFC cannot assure the tracking error of sprung mass displacement within the predefined boundary. Besides, from Fig. 4, the proposed method can enhance passenger comfort since it can provide the smallest acceleration in comparison with the other methods. Results showed that the RMS acceleration value is reduced by 70.6% compared to the passive suspension.

To evaluate the objectives of road handling and handling stability, we can observe that the constraints discussed (23) and (24) are satisfied as shown in Figs. 5 - 6. With the help of PPF, the proposed control can regulate the chassis displacement and ensure the magnitude of RSD within the limit value as Fig. 5. Moreover, driving safety can be guaranteed because the RTF value is smaller than 1. In general, by compensating for unknown parameters and external disturbances, the proposed method can improve the suspension objectives more than the other methods. To assess the effectiveness of the control signal, the simulation results are displayed in Fig. 7. We can see that the developed scheme with the fuzzy observer and CFC technique requires the smallest signal voltage in comparison with the other controllers. Although the back-CFC can eliminate the explosion of complexity issue of the traditional backstepping, it needs more energy to compensate for uncertain parameters. By applying the serial-parallel estimation technique, the recommended controller can improve the suspension performance despite unmeasured states and non-ideal actuator characteristics.

V. CONCLUSION

In this study, the serial-parallel approximation technique is introduced into the control algorithm of the pneumatic suspension to improve the estimation accuracy for unmeasured states. By employing fuzzy estimation, the effects of uncertain parameters, unmodeled dynamics, and unknown actuator characteristics are compensated to increase the control performance. Besides, the CFC technique was constructed into the control design to effectively reduce the explosion of complexity issue of the traditional backstepping. With PPF constraint, the proposed controller not only limits the tracking error of chassis displacement to improve the ride comfort but also guarantees driving safety and handling stability under the presence of parametric uncertainties and non-ideal actuator characteristics. Results show that the proposed method can decrease the RMS acceleration value by 70.6% to get passenger comfort. Generally, the developed approach can solve the suspension objectives and may provide a promising method for the automotive industry. Further studies will focus on the optimal control method for the pneumatic suspension that can be applied in practical implementation.

REFERENCES

[1] H. Kim and H. Lee, "Height and leveling control of automotive air suspension system using sliding mode approach," *IEEE Trans. Veh. Technol.*, vol. 60, no. 5, pp. 2027–2041, Jun. 2011.

[2] Y. Liu, Q. Zeng, L. Liu, and S. Tong, "An adaptive neural network controller for active suspension systems with hydraulic actuator," *IEEE Trans. Syst., Man, Cybern., Syst.*, vol. 50, no. 12, pp. 5351–5360, Dec. 2020.

[3] D. Ning, H. Du, N. Zhang, S. Sun, and W. Li, "Controllable electrically interconnected suspension system for improving vehicle vibration performance," *IEEE/ASME Trans. Mechatronics*, vol. 25, no. 2, pp. 859–871, Apr. 2020.

[4] C. M. Ho, D. T. Tran, and K. K. Ahn, "Adaptive sliding mode control based nonlinear disturbance observer for active suspension with pneumatic spring," *J. Sound Vib.*, vol. 509, Sep. 2021, Art. no. 116241.

[5] H.-Y. Chen and J.-W. Liang, "Adaptive wavelet neural network controller for active suppression control of a diaphragm-type pneumatic vibration isolator," *Int. J. Control, Autom. Syst.*, vol. 15, no. 3, pp. 1456–1465, Jun. 2017.

[6] H. Pan, W. Sun, X. Jing, H. Gao, and J. Yao, "Adaptive tracking control for active suspension systems with non-ideal actuators," *J. Sound Vib.*, vol. 399, pp. 2–20, Jul. 2017.

[7] H. Pan and W. Sun, "Nonlinear output feedback finite-time control for vehicle active suspension systems," *IEEE Trans. Ind. Informat.*, vol. 15, no. 4, pp. 2073–2082, Apr. 2019.

[8] Y. Liu, Y. Zhang, L. Liu, S. Tong, and C. L. P. Chen, "Adaptive finite-time control for half-vehicle active suspension systems with uncertain dynamics," *IEEE/ASME Trans. Mechatronics*, vol. 26, no. 1, pp. 168–178, Feb. 2021.

[9] J. Pan, W. Li, and H. Zhang, "Control algorithms of magnetic suspension systems based on the improved double exponential reaching law of sliding mode control," *Int. J. Control, Autom. Syst.*, vol. 16, no. 6, pp. 2878–2887, Dec. 2018.

[10] V. S. Deshpande, P. D. Shendge, and S. B. Phadke, "Nonlinear control for dual objective active suspension systems," *IEEE Trans. Intell. Transp. Syst.*, vol. 18, no. 3, pp. 656–665, Mar. 2017.

[11] W. Li, Z. Xie, J. Zhao, P. K. Wong, and P. Li, "Fuzzy finite-frequency output feedback control for nonlinear active suspension systems with time delay and output constraints," *Mech. Syst. Signal Process.*, vol. 132, pp. 315–334, Oct. 2019.

[12] J. J. Rath, M. Defoort, C. Sentouh, H. R. Karimi, and K. C. Veluvolu, "Output-constrained robust sliding mode based nonlinear active suspension control," *IEEE Trans. Ind. Electron.*, vol. 67, no. 12, pp. 10652–10662, Dec. 2020.

[13] B. Lin and X. Su, "Fault-tolerant controller design for active suspension system with proportional differential sliding mode observer," *Int. J. Control, Autom. Syst.*, vol. 17, no. 7, pp. 1751–1761, Jul. 2019.

[14] H. Pang, X. Zhang, and Z. Xu, "Adaptive backstepping-based tracking control design for nonlinear active suspension system with parameter uncertainties and safety constraints," *ISA Trans.*, vol. 88, pp. 23–36, May 2019.

[15] C. P. Bechlioulis and G. A. Rovithakis, "Robust adaptive control of feedback linearizable MIMO nonlinear systems with prescribed performance," *IEEE Trans. Autom. Control*, vol. 53, no. 9, pp. 2090–2099, Oct. 2008.

[16] Y. Huang, J. Na, X. Wu, X. Liu, and Y. Guo, "Adaptive control of nonlinear uncertain active suspension systems with prescribed performance," *ISA Trans.*, vol. 54, pp. 145–155, Jan. 2015.

[17] Y. Liu and H. Chen, "Adaptive sliding mode control for uncertain active suspension systems with prescribed performance," *IEEE Trans. Syst., Man, Cybern., Syst.*, vol. 51, no. 10, pp. 6414–6422, Oct. 2021.

[18] J. Na, Y. Huang, Q. Pei, X. Wu, G. Gao, and G. Li, "Active suspension control of full-car systems without function approximation," *IEEE/ASME Trans. Mechatronics*, vol. 25, no. 2, pp. 779–791, Apr. 2020.

[19] J. A. Farrell, M. Polycarpou, M. Sharma, and W. Dong, "Command filtered backstepping," *IEEE Trans. Autom. Control*, vol. 54, no. 6, pp. 1391–1395, Jun. 2009.

[20] C. M. Ho and K. K. Ahn, "Observer based adaptive neural networks fault-tolerant control for pneumatic active suspension with vertical constraint and sensor fault," *IEEE Trans. Veh. Technol.*, vol. 72, no. 5, pp. 1–14, May 2022.

[21] J. Qiu, K. Sun, I. J. Rudas, and H. Gao, "Command filter-based adaptive NN control for MIMO nonlinear systems with full-state constraints and actuator hysteresis," *IEEE Trans. Cybern.*, vol. 50, no. 7, pp. 2905–2915, Jul. 2020.

[22] C. M. Ho and K. K. Ahn, "Design of an adaptive fuzzy observer-based fault tolerant controller for pneumatic active suspension with displacement constraint," *IEEE Access*, vol. 9, pp. 136346–136359, 2021.

[23] Y. Liu, Q. Zeng, S. Tong, C. L. P. Chen, and L. Liu, "Adaptive neural network control for active suspension systems with time-varying vertical displacement and speed constraints," *IEEE Trans. Ind. Electron.*, vol. 66, no. 12, pp. 9458–9466, Dec. 2019.

[24] Y. Zhang, Y. Liu, Z. Wang, R. Bai, and L. Liu, "Neural networks-based adaptive dynamic surface control for vehicle active suspension systems with time-varying displacement constraints," *Neurocomputing*, vol. 408, pp. 176–187, Sep. 2020.

[25] H. Li, Z. Zhang, H. Yan, and X. Xie, "Adaptive event-triggered fuzzy control for uncertain active suspension systems," *IEEE Trans. Cybern.*, vol. 49, no. 12, pp. 4388–4397, Dec. 2019.

[26] H. Chen, Y. Liu, L. Liu, S. Tong, and Z. Gao, "Anti-saturation-based adaptive sliding-mode control for active suspension systems with time-varying vertical displacement and speed constraints," *IEEE Trans. Cybern.*, vol. 52, no. 7, pp. 6244–6254, Jul. 2022.

[27] W. Wang and S. Tong, "Observer-based adaptive fuzzy containment control for multiple uncertain nonlinear systems," *IEEE Trans. Fuzzy Syst.*, vol. 27, no. 11, pp. 2079–2089, Nov. 2019.

[28] L. Zhang and G. Yang, "Observer-based adaptive decentralized fault-tolerant control of nonlinear large-scale systems with sensor and actuator faults," *IEEE Trans. Ind. Electron.*, vol. 66, no. 10, pp. 8019–8029, Oct. 2019.

[29] L. An and G. Yang, "Secure state estimation against sparse sensor attacks with adaptive switching mechanism," *IEEE Trans. Autom. Control*, vol. 63, no. 8, pp. 2596–2603, Aug. 2018.

[30] B. Liu, M. Saif, and H. Fan, "Adaptive fault tolerant control of a half-car active suspension systems subject to random actuator failures," *IEEE/ASME Trans. Mechatronics*, vol. 21, no. 6, pp. 2847–2857, Dec. 2016.

[31] C. M. Ho, D. T. Tran, C. H. Nguyen, and K. K. Ahn, "Adaptive neural command filtered control for pneumatic active suspension with prescribed performance and input saturation," *IEEE Access*, vol. 9, pp. 56855–56868, 2021.

[32] C. Hua, J. Chen, Y. Li, and L. Li, "Adaptive prescribed performance control of half-car active suspension system with unknown dead-zone input," *Mech. Syst. Signal Process.*, vol. 111, pp. 135–148, Oct. 2018.
[33] M. Zhang and X. Jing, "A bioinspired dynamics-based adaptive fuzzy SMC method for half-car active suspension systems with input dead zones and saturations," *IEEE Trans. Cybern.*, vol. 51, no. 4, pp. 1743–1755, Apr. 2021.
[34] J. Ma, S. S. Ge, Z. Zheng, and D. Hu, "Adaptive NN control of a class of nonlinear systems with asymmetric saturation actuators," *IEEE Trans. Neural Netw. Learn. Syst.*, vol. 26, no. 7, pp. 1532–1538, Jul. 2015.
[35] J. Yu, L. Zhao, H. Yu, C. Lin, and W. Dong, "Fuzzy finite-time command filtered control of nonlinear systems with input saturation," *IEEE Trans. Cybern.*, vol. 48, no. 8, pp. 2378–2387, Aug. 2018.
[36] S. Tong and Y. Li, "Adaptive fuzzy output feedback control of MIMO nonlinear systems with unknown dead-zone inputs," *IEEE Trans. Fuzzy Syst.*, vol. 21, no. 1, pp. 134–146, Feb. 2013.
[37] L.-X. Wang, "Stable adaptive fuzzy control of nonlinear systems," *IEEE Trans. Fuzzy Syst.*, vol. 1, no. 2, pp. 146–155, May 1993.
[38] W. Dong, J. A. Farrell, M. M. Polycarpou, V. Djapic, and M. Sharma, "Command filtered adaptive backstepping," *IEEE Trans. Control Syst. Technol.*, vol. 20, no. 3, pp. 566–580, May 2012.

CONG MINH HO received the B.S. degree from the Department of Mechanical Engineering, Ho Chi Minh City University of Technology, Ho Chi Minh City, Vietnam, in 2008, the M.S. degree from the Department of Mechanical Engineering, Ho Chi Minh City University of Technology and Education (HCMUTE), Vietnam, in 2018, and the Ph.D. degree from the University of Ulsan, in 2022.

He is currently a Lecturer with the Faculty of Mechanical Engineering, HCMUTE. His research interests include adaptive control, fluid power control, and active suspension systems.

KYOUNG KWAN AHN (Senior Member, IEEE) received the B.S. degree from the Department of Mechanical Engineering, Seoul National University, in 1990, the M.Sc. degree in mechanical engineering from the Korea Advanced Institute of Science and Technology, in 1992, and the Ph.D. degree from the Tokyo Institute of Technology, in 1999.

He is currently a Professor with the School of Mechanical Engineering, University of Ulsan, Ulsan, South Korea. His research interests include the design and control of smart actuator using the smart material, fluid power control and active damping control, and renewable energy. He is an Editor of *IJCAS*, and an editorial board of *Renewable Energy*, *Actuators*, and *Journal of Engineering*.